Computational Materials Science 110 (2015) 281–286

Contents lists available at ScienceDirect

Computational Materials Science

journal homepage: www.elsevier.com/locate/commatsci

DEM–FEA estimation of pores arrangement effect on the compressive Young's modulus for Mg foams

L. Pérez [a], S. Lascano [b], C. Aguilar [c], D. Estay [b], U. Messner [d], I.A. Figueroa [e], I. Alfonso [e,*]

[a] Department of Mechanical Engineering, Advanced Center for Electrical and Electronic Engineering (Basal Project FB0008), Universidad Técnica Federico Santa María, Av. España 1680, Casilla 110-V, Valparaíso, Chile
[b] Department of Mechanical Engineering, Universidad Técnica Federico Santa María, Av. España 1680, Casilla 110-V, Valparaíso, Chile
[c] Department of Metallurgical and Materials Engineering, Universidad Técnica Federico Santa María, Av. España 1680, Casilla 110-V, Valparaíso, Chile
[d] Department of Mechanical Engineering, University of Applied Sciences Offenburg, Badstraße 24, 77652 Offenburg, Germany
[e] Instituto de Investigaciones en Materiales, Universidad Nacional Autónoma de México, Circuito Exterior SN, Ciudad Universitaria, C.P. 04510, Del. Coyoacán, México, DF, Mexico

ARTICLE INFO

Article history:
Received 1 June 2015
Received in revised form 17 August 2015
Accepted 19 August 2015
Available online 5 September 2015

Keywords:
Foam
Mg
FEA
DEM
Random pores

ABSTRACT

This work reports the study of the effect of the pore arrangement on the compressive behavior of Mg foams with regular pore size and porosities ranging from 25% to 45%. Pore arrangements were modeled using Finite Element Analysis (FEA), with random and ordered models, and compared to the estimations obtained for a previous work. The coordinates of the random pore arrangements were firstly generated using Discrete Element Method (DEM), and used in a second stage for modeling the pores by FEA. Estimations were also compared to the experimental results for Mg foams obtained by means of powder metallurgy. Results show important drops in the Young's moduli as the porosity increases for both, experimental results and FEA estimations. Estimations obtained using ordered pore arrangements presented significant differences when compared to the estimations acquired from models with random arrangements. The randomly arranged models represent more accurately the real topologies of the experimental metallic foams. The Young's moduli estimated using these models were in excellent agreement with the experiments, whilst the estimations obtained using ordered models presented relative errors significantly higher. The importance of the use of more realistic FEA models for improving the predicting ability of this method was probed, for the study of the mechanical properties of metallic foams.

1. Introduction

The study of metallic foams has increased in an important way due to their exceptional mechanical, thermal, acoustic, electrical and chemical properties [1,2], presenting a unique combination of physical and chemical properties derived from their structure [3]. One of the most important manufacturing methods for metallic foam production is the conventional powder metallurgy (PM) incorporating a removable Space Holder Phase (SHP) [4,5]. This phase can be removed by the Sintering and Dissolution Process (SDP), which is a useful method for the production of Mg foams with good mechanical properties and interconnected pores [6]. In order to optimize the design process, depending on the desired properties and applications of the foams, it is very important to have predictions of their mechanical behavior before their fabrication. Among the most important properties to be determined for the metallic foams is the elastic modulus, i.e. comparing the estimations with the experimental results and with the results obtained from other models reported in literature [7,8]. The predictions are highly important for the analysis of new products especially in the case of Mg foams manufactured using a SHP, where the resulting porosity is highly dependent on the metallic powder-space holder particle mixture. Due to its modeling capability, Finite Element Analysis (FEA) is one of the methods used to predict foam properties, being able to model different geometries and analyze their effect on the mechanical properties. A wide variety of pore models have been used for the analysis of foams. Nevertheless, a great percentage of these models use ordered pore arrangements usually not matching the real foam topology [7,9], leading over-predict the foam strength. It is important to remark that the validity of the predictions mainly depends on the proximity of the model to the real foam topology. The over predictions can reach relative errors up to 40% for uniform models when compared to randomized models, as the observed by Meguid et al. [10]. In real cellular structures, foam topology is typically aperiodic,

* Corresponding author. Tel.: +52 5556223857.
E-mail address: ialfonso@unam.mx (I. Alfonso).

http://dx.doi.org/10.1016/j.commatsci.2015.08.042
0927-0256/

non-uniform and disordered. Therefore, modeling of imperfections and randomness that exist in real foam structures is a challenge. If these features are not represented, properties as Young's modulus are over estimated. That is why some works have modeled the porosity using random arrangements for the pores, being more realistic and recommended for foams obtained using PM, where the porosity depends on the metallic powder-space holder composite induced after mixed. These models with disordered pore networks are quite close to the real random 3-D porous structure of the foams, and yield more accurate estimations [11]. Due to the fact that the existing models of the foams (as the presented in Cadena et al. [7], and in Rojek and Oñate [12]) over predict the mechanical properties of foams, it is therefore necessary to have a better foam model. In order to create these models, the first stage is to generate a model of randomly distributed spheres into a certain geometry, e.g. cylinder, which can be achieved via a computer aided design (CAD) software package using script commands. The pores can be modeled as spheres in order to make easier the modeling process, besides the use of this geometry delivers good estimations [7,8]. The number of spheres, their sizes, and the distance between their centers control the porosity percentage and interconnection. In a second stage, the pores are generated by deleting the spheres volume from the container volume [11]. With the use of the Discrete Element Method (DEM), randomly distributed particles can be modeled, and can also be transformed into pores in a second stage. DEM is a family of numerical methods for computing the motion and effect of a large number of small particles. Originally developed by Cundall and Strack [13], it has proven to be a powerful and versatile numerical tool for modeling the behavior of granular and particulate systems [14,15]. DEM operation consists of three principal computational steps: (i) calculation of the contact forces between particles; (ii) integration of equations of motion in order to spot the displacements of the particles; and (iii) contact detection, where new contacts are identified and broken contacts are removed [16]. Within DEM it is assumed that a solid material can be represented as a collection of rigid particles interacting among themselves in the normal and tangential directions [12]. Hence, the final position of the SHP in the mixing process of the metallic powder-space holder mixture used in the manufacturing process of the metallic foams could be simulated using DEM, similar as granular structures modeled by Nitka et al. [17]. This mixture commonly presents agglomeration of the space holder particles, provoking the subsequent interconnection of the pores. DEM can be used in order to obtain just the center of each pore (modeled fist as spheres), controlling the distance between these centers for modeling in a second stage both not connected and interconnected pores. The use of DEM provides several advantages; one of them could be reduction in computer requirements. For a random insertion of particles using a computer program, one of the most important parameters that must be controlled is the distance between the centers of the spheres. Besides this, an algorithm for generating these randomly distributed coordinates is needed [11]. Due to convergence problems, these methods for generating points are computationally time consuming, as they imply a number of operations proportional to N^2, where N is the number of particles. For instance the convergence rate of any method which convergence speed is $1/\sqrt{N}$, tends to perform rather slow, therefore, any state of the art DEM algorithm used for this purpose would be more efficient, as reported in ref [18]. DEM–FEA combination can replicate the agglomeration process of pores, which is very useful if we take into account that for receiving estimations closer to experimental values the pores must not only be randomly distributed in the matrix but also interconnected [19]. Based on the above, the aim of the present work is to generate randomly arranged porous networks that better reproduce the random topology of metallic foams with the focus on improvement of the porosity-properties correlation of models with regularly distributed porosity, as the reported in a previous work for these foams [7]. To validate these models, the compressive Young's moduli of the foams were estimated using FEA, and compared to the experimental results for Mg foams obtained by the SDP route.

2. Experimental

Mg foams with different porosities were obtained by means of powder metallurgy using as SHP spherical carbamide (CH_4N_2O) (99% purity, Sigma Aldrich) with diameters in the range from 1 mm to 2 mm. The metal powder used for processing the foams was Mg (99.5% purity, Alfa Aesar) with diameters ranging from 400 μm to 500 μm. The mixture SHP-metal powder was introduced into a steel mold and uni-axially pressed at 300 MPa to produce cylindrical compacts with 13.0 mm in diameter and 15.0 mm in length. The carbamide fraction of the green compact formed at this stage was dissolved by immersion in a water bath at 25 °C for 1 h, revealing the spherical pores. Finally, the sintering process was carried out at 620 °C under an Ar atmosphere. Optical macrographies of the cylindrical foams were prepared to analyze the foams topology. The Young's moduli of the specimens, measured by means of compression tests, were conducted on an Instron 1125-5500R materials testing machine with a crosshead speed of 0.1 mm/min, according to the ASTM E9-09. Mg and carbamide were mixed in proportions of 80–20, 70–30 and 60–40 (in wt.%), respectively. The densities of the foams were determined using the conventional equation for density, while the volumes were measured by the Archimedes principle. The real foams porosities (P_f, in percentage) were determined through the following equation [20]:

$$P_f = \left(1 - \rho_f/\rho_{Mg}\right) \times 100 \quad (1)$$

where ρ_{Mg} is the Mg density (1.74 g/cm^3) and ρ_f is the foam density.

3. Modeling and simulation

3.1. Generation of random distributions using DEM

This process consists of ascertaining the behavior of spheres immersed in a continuous medium, in our particular case, having the shape of a cylinder. Open source DEM particle simulation software LIGGGHTS® [21] was used in order to generate randomly distributed particles, being the initial stage of the modeling process. These results are post-processed in order to generate an ANSYS 14.5 Design Modeler script, using the obtained random coordinates to locate the pores and create the CAD model for the foam. A very important aspect of this procedure is locating pores at the surface of the foam as in real specimens. This was achieved by inserting particles/pores with a geometry slightly greater than that required. Depending on the porosity percentage, a certain number of particles were inserted into a cylindrical geometry according to the dimensions of the specimen (13.0 mm in diameter and 15.0 mm in length). The conditions of the particles insertion were: high velocity, high coefficient of restitution and low Young's modulus, into a space with gravity near to zero. These conditions were selected just in order to generate a high interaction between the particles and to get the desired random distribution, and not for simulating the interaction between the SHP and the metallic particles during the mixing process. This allows to use the obtained coordinates for modeling any metallic foam, regardless the type of SHP used. Some examples of particles distribution at different times are shown in Fig. 1a–c. As can be observed, the interaction

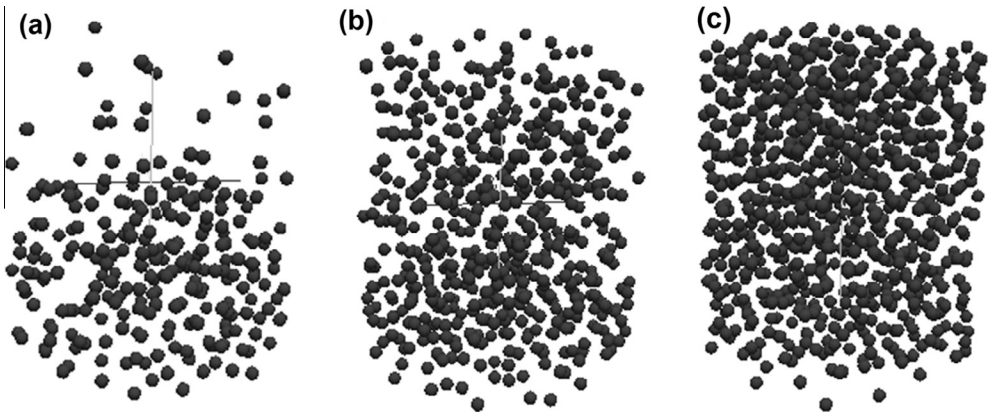

Fig. 1. Particles distribution generated using DEM for a specimen with a final porosity of 31% at different stages of the interaction process: (a) initial distribution, (b) distribution for half interaction time, and (c) final distribution of the inserted particles.

between the particles leads after the final process to the fact that the particles are distributed not only at the bottom of the container but also within the complete geometry.

3.2. Finite elements model

The finite elements models consisted on cylindrical specimens of 13 mm in diameter and 15 mm in length, with porosities ranging from 25% to 51%, in order to match with the characteristics of the experimental foams. The FEA models included spherical pores of 1.5 mm in diameter, which were distributed using two different criteria: (i) regularly distributed, completely generated using ANSYS 14.5 FEA, according to a previous work [7]; and (ii) randomly distributed generated using DEM, prepared for the FEA analyses using ANSYS 14.5. Fig. 2a and b shows the modeled cylindrical foams with porosities of 31% (corresponding to the generated particles observed in Fig. 1c) and 47%, respectively, engendered through DEM–FEA combination (named as DEM–FEA 1). As can be observed, the distributions of the porosities are random. Besides, the pores present important interconnections. A second case (named as DEM–FEA 2) is depicted in Fig. 2c, for a model with a porosity of 51%, where a higher interaction between the particles was programmed and thus, a higher agglomeration and interconnection of pores was obtained. These two cases of study are representative of the final positions of the SHP after the mixing process for manufacturing the foams (corresponding to the final site of the pores). Otherwise, the models generated using FEA software ANSYS 14.5 present regular distributions, as can be observed in Fig. 2d for the model with a porosity of 45%. For the regular models poor interconnections between the pores have been achieved (see the interconnection of some pores at the top in Fig. 2d), a fact that will be further analyzed.

As above-mentioned, the pore agglomeration is also an important characteristic, which is incorporated in the models generated using DEM, in an initial stage. This is what causes the pore interconnections, this phenomenon is usually observed in foams produced by the SHP [7,22] and it has been also observed on many other foams [11,23]. Fig. 3a–c shows cases of the already commented interconnected porosity of DEM models for foams with porosities of 31% (Fig. 3a) and 47% (Fig. 3b) in case 1; and with a porosity of 51% (Fig. 3c) in case 2. As can be observed, the increase in the total porosity results in a higher interconnection between the pores. Besides, a higher pore interconnection was obtained for case 2 when compared to case 1. In FEA models, as also observed in our previous work [7], pores interconnections were poor. For these regular models the unit cells are modeled in such way that the pores are at the same distance, and even for the case of the model with the highest porosity (45%), it was possible to model the pores without an important interconnection. Interconnected pores allow it to get models much closer to the real foams topology, which is an important fact for improving the predicting ability of FEA. These models will be compared with the experimental foams in order to establish their validity. It is worth mentioning that the low interconnection between the pores in the regular models could be one of the most important causes of the Young's moduli over predictions.

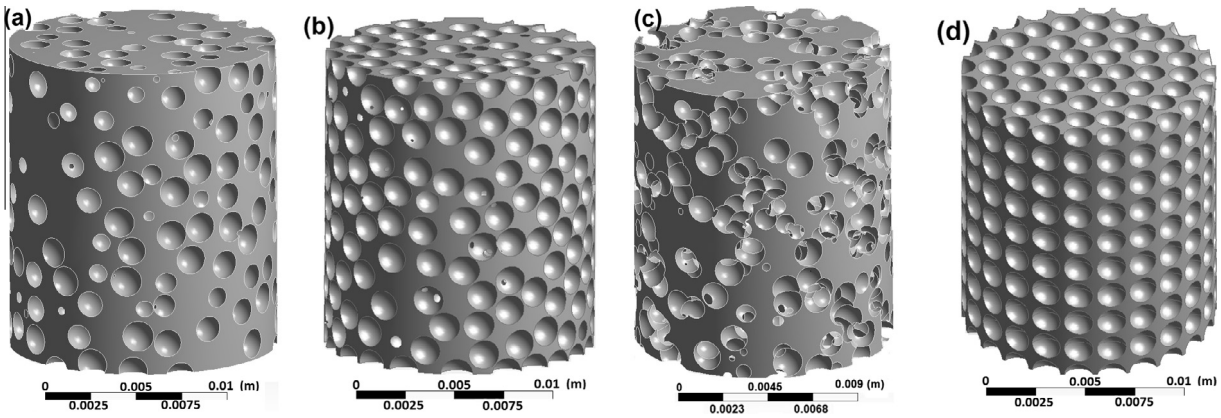

Fig. 2. DEM–FEA models of foams with randomly ordered porosities of: (a) 31% (case 1), (b) 47% (case 1), (c) 51% (case 2); and (d) FEA model with a regularly distributed porosity of 45%.

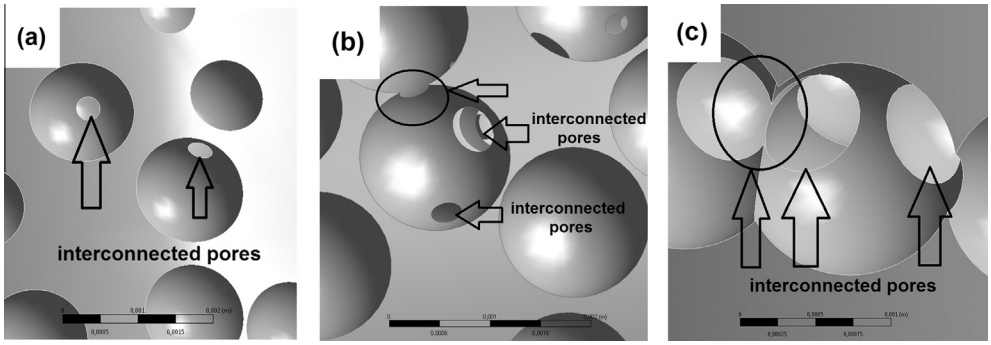

Fig. 3. DEM–FEA models of foams with randomly ordered porosities: (a) 31% case 1, (b) 47% case 1, and (b) 51% case 2. The interconnection of the pores is clearly observed.

3.3. Simulation

The Young's moduli of the metallic foams with different porosities were uni-axially estimated when applying equivalent compressive stresses on the upper end nodes of the cylindrical specimens. The conditions were replicated from a previous work [7] in order to compare the obtained estimations with the experimental measurements. The SOLID187 3-D 10-node tetrahedral structural solid element was employed for meshing with an element size of 0.00025 mm. The coupled-node boundary condition (keeping the nodes in the same plane) was used for the upper face of the cylinder. This condition is applied since the presence of pores results in un-even surfaces, and therefore, the deformation measurement was difficult to define. Young's modulus can be obtained from the response of the compression test, and along the z-axis (E_z), it can be determined by:

$$E_z = \frac{\sigma_z}{\varepsilon_z} \tag{2}$$

where σ_z and ε_z are the stress and the strain in z-axis, respectively. The displacement of the cylinder in z-axis (u_z) is measured from the FEA estimations, and used for the strain determination:

$$\varepsilon_z = \frac{u_z}{L_z} \tag{3}$$

where L_z is the original height of the cylindrical specimen. The Young's modulus (1.5 GPa) and Poisson's Ratio (0.29) used for simulations were obtained from the results of the compressive test of a specimen sintered without space holder particles.

4. Results and discussion

The real porosities of the experimentally produced foams (calculated using Eq. (1)) were 31%, 42% and 51%, while their densities were 1.18, 1.07 and 0.94 g/cm^3, respectively. Fig. 4a–c shows optical macrographs of these foams. As it can be observed, pores with random distributions are presented, showing that using the models initially generated by DEM (already observed in Fig. 2a and b) does enhance the reproduction of topologies of the experimental foams. In order to analyze the pores interconnection, SEM micrographies were obtained. Fig. 4d shows the interconnectivity between the pores for the foam with 60% Mg and 40% carbamide, where the porosity and the interconnection between the pores was the highest (clearly observed in Fig. 4c). Table 1 presents the percentage of pores that are interconnected for the models and the experimentally obtained foams. As can be observed, the models obtained using DEM have interconnectivities very close to the values of the experimental foams, whilst the models generated using

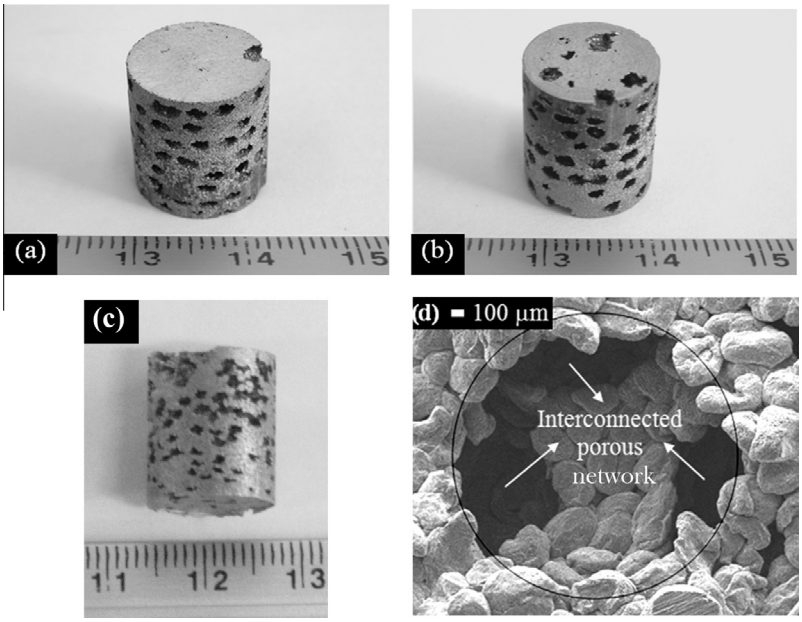

Fig. 4. Macrographies of Mg foams with porosities of: (a) 31%, (b) 42% and (c) 51% (scales in mm). (d) SEM micrography of the foam with a porosity of 51% showing the interconnection between pores.

Table 1
Interconnected pores (in %) for the models and the experimental foams.

	Foam porosity (%)		
	25	35	45
FEA model	0	0	50
DEM model 1	8	27	86
DEM model 2	10	31	94
Experimental foams	6	35	89

FEA shows lower interconnectivities, being zero for the foams with porosities of 25% and 35%.

These results showed that porosities regularly modeled, as already analyzed by Cadena et al. [7], are mismatched to the experimental results, a fact that significantly changed the predictions obtained by the FEA models. An important increase in the pores interconnectivity with porosity is one of the characteristics that must have foam models. It is expected that the use of the DEM models allow improving the predicting ability of FEA.

The graphical response of the models to the distributed applied loads for the foams with different porosities can be observed in Fig. 5a–d. This figure shows that directional displacements in *Z* (maximum displacement being negative) are directly proportional to the porosity for both random (Fig. 4a–c) and regular (Fig. 4d) porosity distributions. As is observed, the regular models presented lower displacements than the random ones, which showed that the modeled foams are stiffer when no interconnection within pores is included.

FEA estimated results and experimental values for the Young's moduli depending on the porosity are compared in Fig. 6a. As observed, the Young's modulus significantly decreases when the porosity increases for both, predictions and experimental values. Nevertheless, it can be clearly observed that the FEA estimations using the DEM random models (for cases 1 and 2) are very close to the experimental results, decreasing in similar ways. The Young's modulus for the experimental foam with a porosity of 25% is 0.79 GPa, decreasing to 0.29 GPa for the foam with a porosity of 45%. For the DEM–FEA random model the decrease was from 0.78 GPa to 0.30 GPa. No significant differences were observed for cases 1 and 2. Otherwise, for the estimations obtained by Cadena et al. [7], and for the replication of the regular distributions used in the present work, the decreases were different compared to the experimental results, i.e. decreasing only to 0.54 GPa. Fig. 6b shows the relative errors of these values as a function of the experimental results. It can be clearly observed that the DEM–FEA models estimations are very close to the experimental results, obtaining the lowest errors (maximum 9.7%). The resulting small relative errors could be attributed to the fact that the modeled topology is close to the real one, increasing the interconnection between the pores with the increment in porosity. Then, although

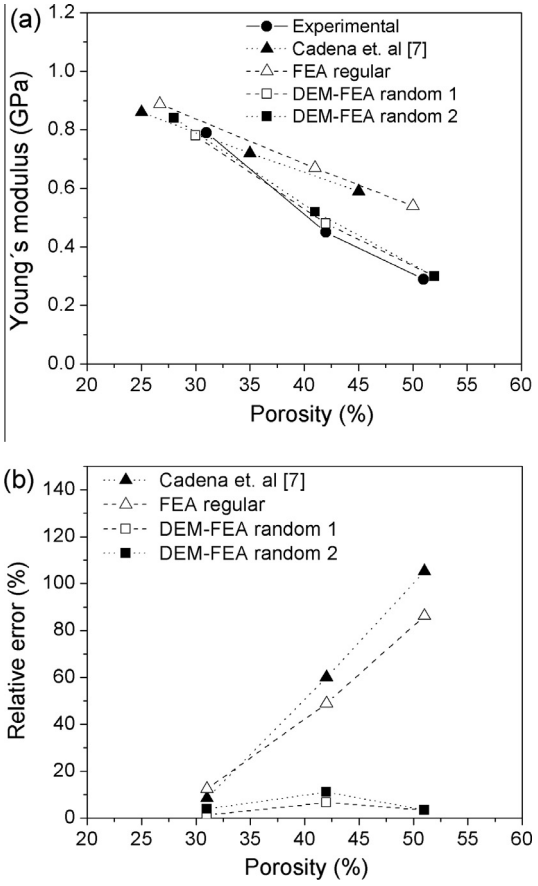

Fig. 6. (a) Compressive Young's modulus variation, and (b) their relative errors as a function of porosity (%).

for low porosities the relative errors between FEA estimations using regular pore distributions and experimental values were low (~10%), these values significantly increased when the porosity increases. The maxima relative errors of 105.17% Cadena et al. [7], and 86.3% (regular distributions used in the present work) were obtained for the foam with the highest porosity, showing that the selected models were not accurate enough. As mentioned above, all the experimental foams present interconnections between pores. At low porosities, the quantity of the space holder particles used in the manufacturing process is low, and as a consequence, the interaction between the space holder particles is low, and the interconnection of the obtained pores is not that high as in the case of the manufacturing process with a higher quantity of space holder particles, where the maximum interconnection between the pores was reached. As a result, the real topology of

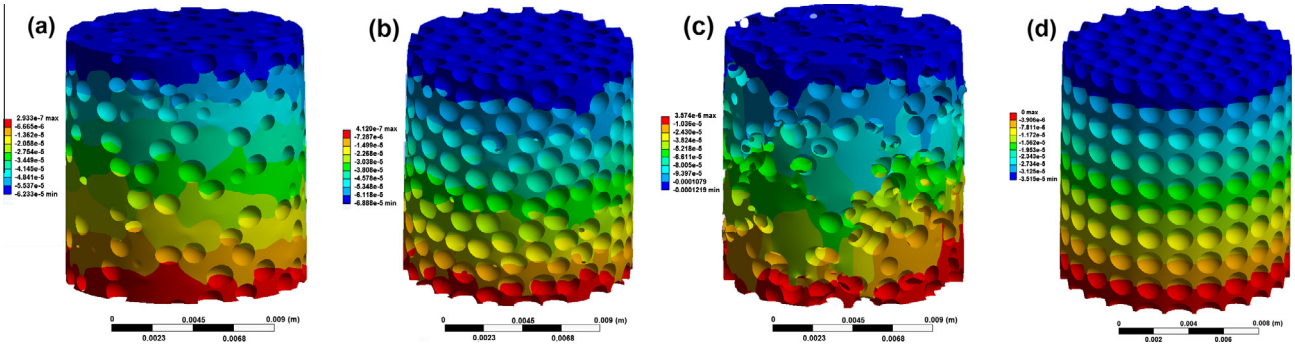

Fig. 5. Directional deformation in *Z* (in m) under compression for the Mg foam random models with porosities of: (a) 31% case 1, (b) 47% case 1, and (b) 51% case 2; and regular model with a porosity of 45%.

the foams is markedly different compared to the FEA regular models. For regular models the pores are at the same distance and present low interconnection. These different topologies led to important mismatches between the experimental results and FEA estimations, over-predicting the foam strength when a regular and not interconnected porous network was modeled. These results showed the importance of the DEM–FEA combination for the study of foams, predicting in a rather accurate way their compressive behavior. The use of DEM in an initial stage allowed taking into account not only the porosity percentage, size and shape of the pores, but also their random distribution, originated during the manufacturing process. This helped to get predictions closer to the experimental results than the models that included regular distributions of the pores. The selection of the foam topology has demonstrated to be an essential variable for correcting estimations.

5. Conclusions

In this work, three-dimensional models were used in order to predict the compressive behavior of Mg foams with porosities ranging from 25% to 51%. Results showed that the use of FEA regular models, with low interconnectivity between the pores, resulted in high relative errors for the foams with high porosities, over-predicting the strength of the experimentally obtained foams. The introduction of random models generated using a DEM–FEA combination made it possible to realize a more realistic topology of the modeled foams, even for high porosities, where important interconnection between the pores was reached. These random models allowed monitoring important decreases in the differences between estimated and experimental values. DEM demonstrated to be an excellent tool for reproducing the topology of foams using space holders. The selection of the correct foam topology for a model has demonstrated to be an essential variable for obtaining estimations closer to the experimental results.

Acknowledgements

The authors would like to acknowledge the financial support from SENER–CONACYT 151496 and UNAM PAPIIT TA100114 for funding the Project. L. Pérez acknowledges the financial support from the Chilean Agency CONICYT (FONDECYT Project 1140583).

References

[1] J. Banhart, M.F. Ashby, N.A. Fleck, Metal Foams and Porous Metal Structures, Verlag MIT Publishing, Bremen, 1997.
[2] L.J. Gibson, M.F. Ashby, Cellular Solids: Structure and Properties, second ed., Cambridge University Press, Cambridge, UK, 1997.
[3] G.J. Davies, S. Zhen, J. Mate. Sci. 18 (1983) 1899, http://dx.doi.org/10.1007/BF00554981.
[4] M.F. Ashby, A.G. Evans, N.A. Fleck, L.J. Gibson, J.W. Hutchinson, H.N.G. Wadley, Metal Foams: A Design Guide, Butterworth-Heinemann, USA, 2000.
[5] J. Banhart, Prog. Mater. Sci. 46 (2001) 559, http://dx.doi.org/10.1016/S0079-6425(00)00002-5.
[6] J.O. Osorio-Hernández, M.A. Suarez, R. Goodall, G.A. Lara-Rodriguez, I. Alfonso, I.A. Figueroa, Mater. Des. 64 (2014) 136–141, http://dx.doi.org/10.1016/j.matdes.2014.07.015.
[7] J.H. Cadena, I. Alfonso, J.H. Ramírez, V. Rodriguez-Iglesias, I.A. Figueroa, C. Aguilar, Comp. Mater. Sci. 91 (2014) 359–363, http://dx.doi.org/10.1016/j.commatsci.2014.04.065.
[8] F.V. Antunes, J.A.M. Ferreira, C. Capela, Finite Elem. Anal. Des. 47 (2011) 78–84, http://dx.doi.org/10.1016/j.finel.2010.09.007.
[9] A. Hasan, Adv. Mater. Sci. Eng. (2010) 12, http://dx.doi.org/10.1155/2010/567390.
[10] S.A. Meguid, S.S. Cheon, N. El-Abbasi, Finite Elem. Anal. Des. 38 (2002) 631–643, http://dx.doi.org/10.1016/S0168-874X(01)00096-8.
[11] M. Kırca, A. Gul, E. Ekinci, F. Yardım, A. Mugan, Finite Elem. Anal. Des. 44 (2007) 45–52, http://dx.doi.org/10.1016/j.finel.2007.08.008.
[12] J. Rojek, E. Oñate, Interact. Multiscale Mech. 1 (1) (2007) 1–31, http://dx.doi.org/10.12989/imm.2008.1.1.001.
[13] P.A. Cundall, O.D. Strack, Geotechnique 29 (1) (1979) 47–65, http://dx.doi.org/10.1680/geot.1979.29.1.47.
[14] R. Dobry, T.T. Ng, Eng. Comput. 9 (2) (1992) 129–143, http://dx.doi.org/10.1234/12345678.
[15] J. Ghaboussi, R. Barbosa, Int. J. Numer. Anal. Met. Geomech. 14 (7) (1990) 451–472.
[16] F.A. Tavarez, M.E. Plesha, Int. J. Numer. Meth. Eng. 70 (4) (2007) 379–404, http://dx.doi.org/10.1002/nme.1881.
[17] M. Nitka, G. Combe, C. Dascalu, J. Desrues, Granular Matter 13 (2011) 277–281, http://dx.doi.org/10.1007/s10035-011-0255-6.
[18] A.A. Munjiza, The Combined Finite-Discrete Element Method, John Wiley & Sons, Chichester, UK, 2004.
[19] P.R. Marur, Finite Elem. Anal. Des. 46 (2010) 1001–1007, http://dx.doi.org/10.1016/j.finel.2010.07.006.
[20] Y.Y. Zhao, D.X. Sun, Scripta Mater. 44 (2000) 105–110, http://dx.doi.org/10.1016/S1359-6462(00)00548-0.
[21] C. Kloss, C. Goniva, A. Hager, S. Amberger, S. Pirker, Prog. Comput. Fluid Dy. 12 (2012) 140–152, http://dx.doi.org/10.1504/PCFD.2012.047457.
[22] J.A. Gutiérrez-Vázquez, J. Oñoro, Fabricación, propiedades y aplicaciones, Revista de Metalurgia 44 (5) (2008) 457–476, http://dx.doi.org/10.3989/REVMETALM.0751.
[23] K.M. Ryu, J.Y. An, W.S. Cho, Y.C. Yoo, H.S. Kim, Mater. Trans. 46 (2005) 622–625, http://dx.doi.org/10.2320/matertrans.46.622.